Electronic Supplementary Material (ESI) for Inorganic Chemistry Frontiers.

MoS_2@C with S vacancies vertically anchored on V_2C-MXene for efficient lithium and sodium storage

Guilong Liu[a], Ting Zhang[a], Xiaojie Li[a], Jin Li[a], Naiteng Wu[a], Ang Cao[b], Weiwei Yuan[a], Kunming Pan[c, d], Donglei Guo*[a] and Xianming Liu*[a]

[a] Key Laboratory of Function-oriented Porous Materials of Henan Province, College of Chemistry and Chemical Engineering, Luoyang Normal University, Luoyang 471934, Henan, China

[b] Department of Physics, Technical University of Denmark, Lyngby 2800, Denmark

[c] Henan Key Laboratory of High-temperature Structural and Functional Materials, Henan University of Science and Technology, Luoyang 471023, Henan, China

[d] Longmen Laboratory, Luoyang 471023, Henan, China

*Corresponding author: gdl0594@163.com (Donglei Guo); myclxm@163.com (Xianming Liu)

The calculation process for the composition of MoS_2@C: according to **Figure 3i**, the weight loss of MoS_2@C between 200-460 °C and below 200 °C were measured to be 28.7% and 5.0%, respectively. After removing water, the actual weight loss between 200-460 °C was 30.2%, which originated from the oxidation of MoS_2 into MoO_3 and the combustion of carbon. So, 0.1 W_{MoS_2}+ W_C= 30.2%; W_{MoS_2}+ W_C= 100%. Therefore, W_{MoS_2}=77.5%, W_C=22.5%. When heated to 1000 °C, not all MoO_3 sublimated, and the remaining MoO_3 was 4.9% after removing water.

The calculation process for the composition of f-V_2C-MoS_2@C: according to **Figure 3i**, the weight loss of f-V_2C-MoS_2@C between 200-520 °C and below 200 °C were measured to be 28.5% and 8.8%, respectively. After removing water, the actual weight loss between 200-520 °C was 31.2 %, which originated from the oxidation of MoS_2 into MoO_3, the combustion of carbon and the weight change of V_2C-MXene. When heated to 1000 °C, 29.4% of the samples remained, which contained un-sublimated MoO_3 and remained VO_x. So, 0.1 W_{MoS_2}+ W_C+0.084 W_{V_2C} = 31.2%; (4.9/77.5) W_{MoS_2}+ (1-0.084)

W_{V_2C} = 29.4%; W_{MoS_2}+ W_C+ W_{V_2C} = 100% Therefore, W_{MoS_2}=47.1%, W_C=23.9%, W_{V_2C} =29.0%.

$V_2CT_x+O_2 \rightarrow VO_x+CO_2$ (200-600 °C, measured weight loss 8.4%) (S1)

$2MoS_2+7O_2=2MoO_3+4SO_2$ (200-600 °C, weight loss 10%) (S2)

$C+O_2=CO_2$ (400-600 °C, weight loss 100%) (S3)

$MoO_3(s)=MoO_3(g)$ (＞700 °C, weight loss 100%) (S4)

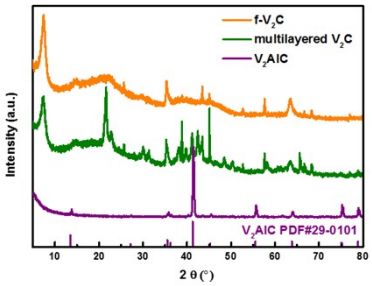

Figure S1 XRD patterns of V_2AlC, multilayered V_2C and f-V_2C

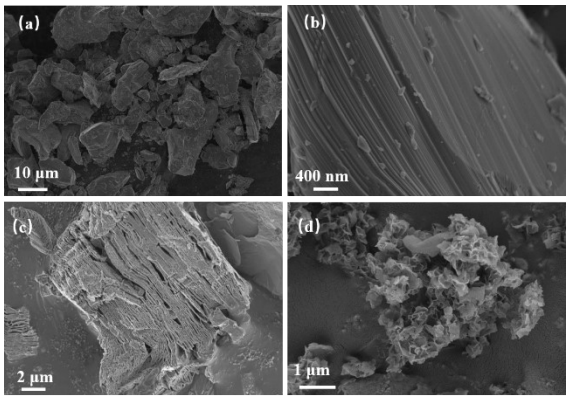

Figure S2 SEM images of (a-b) V_2AlC, (c) multilayered V_2C and (d) f-V_2C

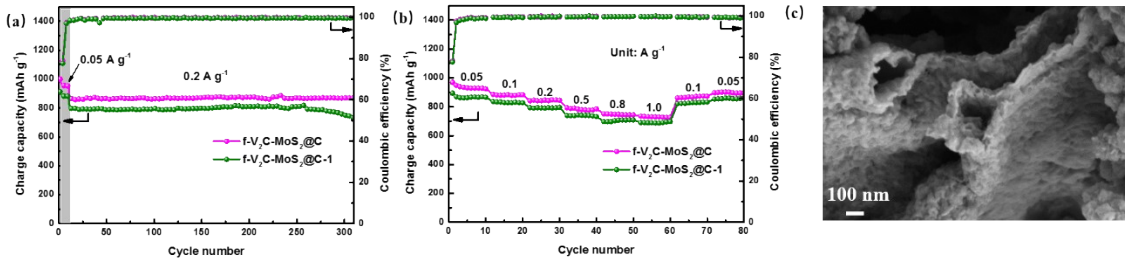

Figure S3 (a) Cyclic and (b) rate performance of f-V_2C-MoS_2@C and f-V_2C-MoS_2@C-1 in LIBs; (c) SEM image of f-V_2C-MoS_2@C-1

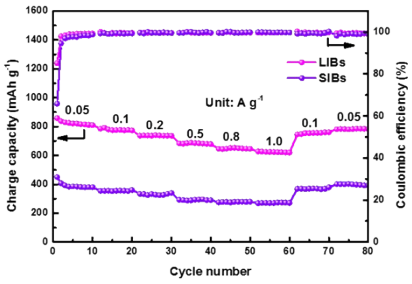

Figure S4 Rate performance of f-V_2C-MoS_2@C with a mass loading of 3 mg cm^{-2}

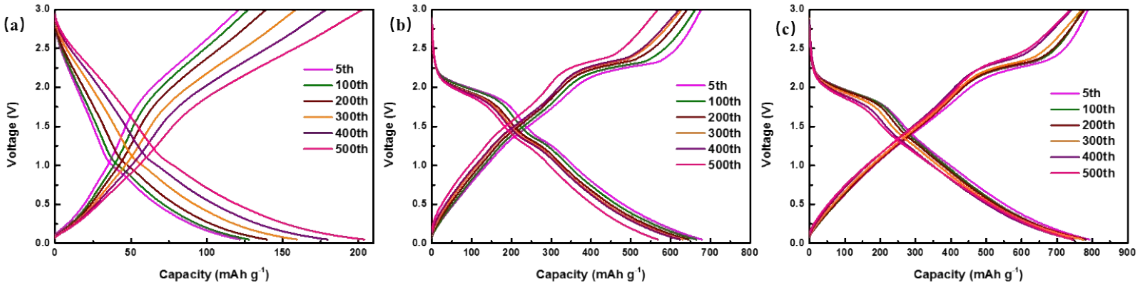

Figure S5 GCD curves of (a) f-V_2C, (b) MoS_2@C and (c) f-V_2C-MoS_2@C in LIBs at 0.5 A g^{-1}

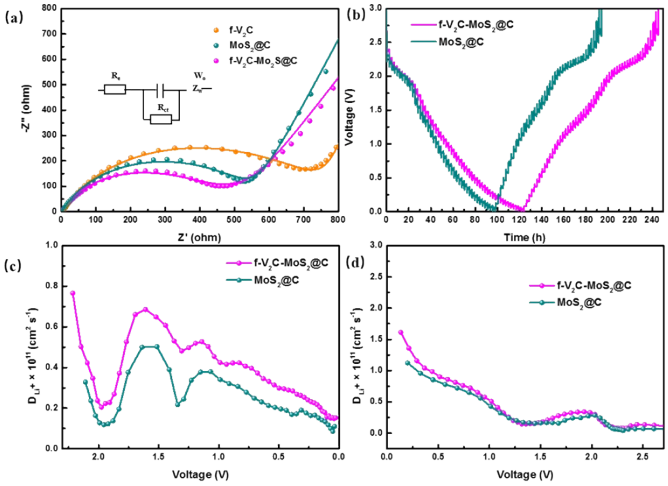

Figure S6 (a) EIS spectra of the three fresh electrodes in LIBs; (b) GITT profiles and the calculated Li^+ diffusion coefficients during (c) discharge and (d) charge process for MoS_2@C and f-V_2C-MoS_2@C in LIBs

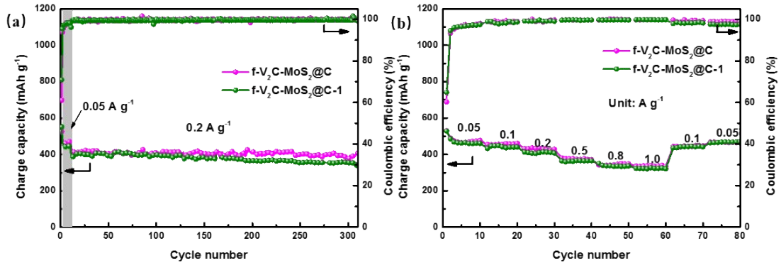

Figure S7 (a) Cyclic and (b) rate performance of f-V_2C-MoS_2@C and f-V_2C-MoS_2@C-1

in SIBs

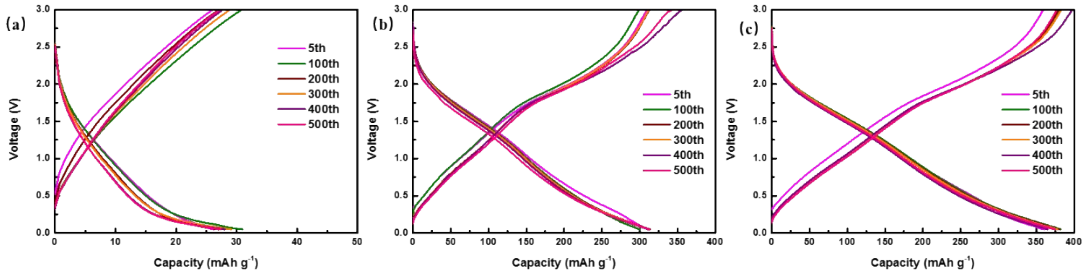

Figure S8 GCD curves of (a) f-V_2C, (b) MoS_2@C and (c) f-V_2C-MoS_2@C in SIBs at 0.5 A g^{-1}

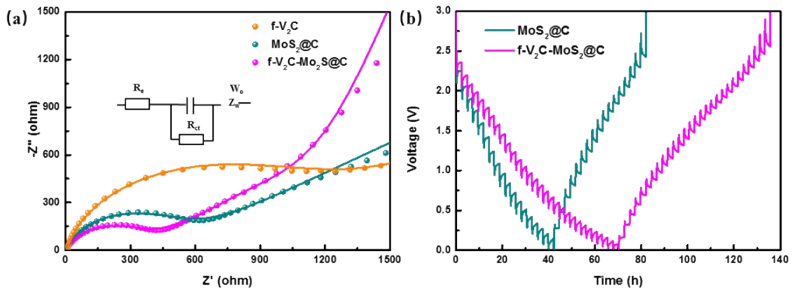

Figure S9 (a) EIS spectra of the three fresh electrodes in SIBs; (b) GITT profiles for MoS_2@C and f-V_2C-MoS_2@C in SIBs

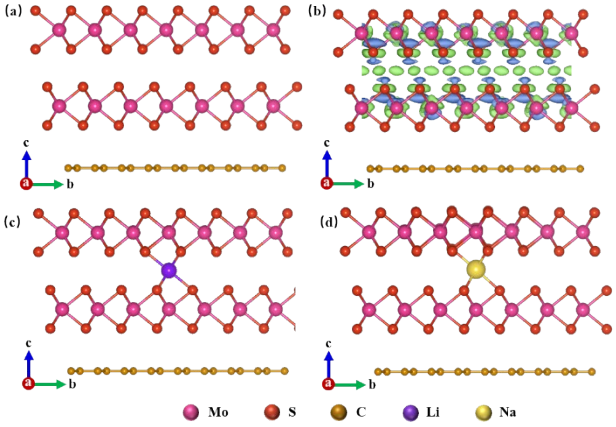

Figure S10 (a) Optimized structure and (b) charge density difference (green and blue isosurfaces showed the accumulation and depletion of electrons region, respectively) of graphene/MoS_2 (001)/MoS_2 (001) model; optimized structures of graphene/ MoS_2 (001)/ MoS_2 (001) model with a (c) Li and (d) Na atom adsorbed

Table S1 Electrochemical performance of state-of-the-art MoS_2-based anode materials in LIBs and SIBs

Materials	Battery system	Cyclic performance	Rate performance	Reference
f-V_2C-MoS_2@C	LIBs	**0.73 Ah g^{-1} after 500 cycles at 0.5 A g^{-1}** **0.87Ah g^{-1} after 300 cycles at 0.2 A g^{-1}**	**0.73 Ah g^{-1} at 1 A g^{-1}**	**This work**
WS_2/MoS_2@C		1.03 Ah g^{-1} after 450 cycles at 0.5 A g^{-1}	0.48 Ah g^{-1} at 1 A g^{-1}	1
MoS_2/C@G		0.67 Ah g^{-1} after 1000 cycles at 0.5 A g^{-1}	0.45 Ah g^{-1} at 1 A g^{-1}	2
c-MoS_2		0.8 Ah g^{-1} after 200 cycles at 0.2 A g^{-1}	0.58 Ah g^{-1} at 1 A g^{-1}	3
MoS_2@C-23		0.63 Ah g^{-1} after 800 cycles at 1 A g^{-1}	0.93 Ah g^{-1} at 1 A g^{-1}	4
MoS_2-PVP@NC		0.61 Ah g^{-1} after 300 cycles at 1 A g^{-1}	0.67 Ah g^{-1} at 1 A g^{-1}	5
MoS_2/SnS		0.99 Ah g^{-1} after 200 cycles at 0.2 A g^{-1}	0.89 Ah g^{-1} at 1 A g^{-1}	6
Ti_3C_2/TiO_2@f-MoS_2		0.49 Ah g^{-1} after 100 cycles at 0.1 A g^{-1}	0.23 Ah g^{-1} at 1 A g^{-1}	7
CNTs@MoS_2/MoO_2		0.58 Ah g^{-1} after 200 cycles at 0.335 A g^{-1}	0.45 Ah g^{-1} at 0.67 A g^{-1}	8
TiO_2@MoS_2 nanotubes		0.62 Ah g^{-1} after 100 cycles at 0.1 A g^{-1}	0.43 Ah g^{-1} at 1 A g^{-1}	9
f-V_2C-MoS_2@C	SIBs	**0.40 Ah g^{-1} after 300 cycles at 0.2 A g^{-1}** **0.37 Ah g^{-1} after 500 cycles at 0.5 A g^{-1}**	**0.34 Ah g^{-1} at 1 A g^{-1}**	**This work**
WS_2/MoS_2@C		0.37 Ah g^{-1} after 280 cycles at 1 A g^{-1}	0.36 Ah g^{-1} at 1 A g^{-1}	1
c-MoS_2		~0.32 Ah g^{-1} after 100 cycles at 0.2 A g^{-1}	0.28 Ah g^{-1} at 1 A g^{-1}	3

MoS_2@C-23		0.33 Ah g^{-1} after 100 cycles at 0.2 A g^{-1}	0.29 Ah g^{-1} at 1 A g^{-1}	4
MoS_2-PVP@NC		0.41 Ah g^{-1} after 200 cycles at 1 A g^{-1}	0.38 Ah g^{-1} at 1 A g^{-1}	5
P-MoS_2@C/CNTP		0.25 Ah g^{-1} after 1000 cycles at 1 A g^{-1}	0.31 Ah g^{-1} at 1 A g^{-1}	10
MX-H-MoS_2@NC		0.26 Ah g^{-1} after 1100 cycles at 1 A g^{-1}	~0.34 Ah g^{-1} at 1 A g^{-1}	11
MoS_2@C		0.40 Ah g^{-1} after 100 cycles at 0.1 A g^{-1}	0.19 Ah g^{-1} at 0.8 A g^{-1}	12
20Nb_2CT_x/MoS_2@CS		0.39 Ah g^{-1} after 800 cycles at 1 A g^{-1}	0.38 Ah g^{-1} at 1 A g^{-1}	13
Dual-phase MoS_2		0.30 Ah g^{-1} after 200 cycles at 0.5 A g^{-1}	0.26 Ah g^{-1} at 1 A g^{-1}	14
HMF-MoS_2		0.38 Ah g^{-1} after 100 cycles at 0.1 A g^{-1}	0.36 Ah g^{-1} at 1 A g^{-1}	15
(MoS_2/CF)@MoS_2@C		0.33 Ah g^{-1} after 1000 cycles at 1 A g^{-1}	0.33 Ah g^{-1} at 1 A g^{-1}	16

Table S2 Impedance parameters of the electrodes after 300 cycles in LIBs

Materials	Fresh electrode		Cycled electrode		
	R_e/Ω	R_{ct}/Ω	R_e/Ω	R_{sf}/Ω	R_{ct}/Ω
V_2C	4.4	698.4	1.7	91.6	58.8
MoS_2@C	2.7	547.5	6.4	26.0	27.2
f-V_2C-MoS_2@C	2.2	395.4	2.3	6.8	7.1

Table S3 Impedance parameters of the electrodes after 300 cycles in SIBs

Materials	Fresh electrode		Cycled electrode		
	R_e/Ω	R_{ct}/Ω	R_e/Ω	R_{sf}/Ω	R_{ct}/Ω
V_2C	6.8	1005	4.8	886.7	903.8
MoS_2@C	1.8	489.9	0.7	63.2	671.9
f-V_2C-MoS_2@C	2.4	358.3	0.2	31.7	255.1

References

1. Y. Rao, J. Wang, P. Liang, H. Zheng, M. Wu, J. Chen, F. Shi, K. Yan, J. Liu, K. Bian, C. Zhang and K. Zhu, Heterostructured WS_2/MoS_2@carbon hollow microspheres anchored on graphene for high-performance Li/Na storage, *Chem. Eng. J.*, 2022, **443**, 136080.
2. B. Lan, X. Zhang, Y. Wang, C. Wei and G. Wen, Constructing highly stable lithium storage materials by improving the bond strength of MoS_2 to graphene via chitosan, *Carbon*, 2022, **192**, 384-394.
3. J. Lin, Y.-H. Shi, Y.-F. Li, X.-L. Wu, J.-P. Zhang, H.-M. Xie and H.-Z. Sun, Confined MoS_2 growth in a unique composite matrix for ultra-stable and high-rate lithium/sodium-ion anodes, *Chem. Eng. J.*, 2022, **428**, 131103.
4. B. Ye, L. Xu, W. Wu, Y. Ye, Z. Yang, J. Ai, Y. Qiu, Z. Gong, Y. Zhou, Q. Huang, Z. Shen, F. Li, T. Guo and S. Xu, Encapsulation of 2D MoS_2 nanosheets into 1D carbon nanobelts as anodes with enhanced lithium/sodium storage properties, *J. Mater. Chem. C*, 2022, **10**, 3329-3342.

5. J. Bai, B. Zhao, X. Wang, H. Ma, K. Li, Z. Fang, H. Li, J. Dai, X. Zhu and Y. Sun, Yarn ball-like MoS_2 nanospheres coated by nitrogen-doped carbon for enhanced lithium and sodium storage performance, *J. Power Sources*, 2020, **465**, 228282.
6. J. Ru, T. He, B. Chen, Y. Feng, L. Zu, Z. Wang, Q. Zhang, T. Hao, R. Meng, R. Che, C. Zhang and J. Yang, Covalent Assembly of MoS_2 Nanosheets with SnS Nanodots as Linkages for Lithium/Sodium-Ion Batteries, *Angew. Chem. Int. Ed.*, 2020, **59**, 14621-14627.
7. X. Zhang, J. Li, L. Han, H. Li, J. Wang, T. Lu and L. Pan, In-situ fabrication of few-layered MoS_2 wrapped on TiO_2-decorated MXene as anode material for durable lithium-ion storage, *J. Colloid Interface Sci.*, 2021, **604**, 30-38.
8. H. Lu, K. Tian, L. Bu, X. Huang, X. Li, Y. Zhao, F. Wang, J. Bai, L. Gao and J. Zhao, Synergistic effect from coaxially integrated CNTs@MoS_2/MoO_2 composite enables fast and stable lithium storage, *J. Energy Chem.*, 2021, **55**, 449-458.
9. J. Li, L. Han, X. Zhang, H. Sun, X. Liu, T. Lu, Y. Yao and L. Pan, Multi-role TiO_2 layer coated carbon@few-layered MoS_2 nanotubes for durable lithium storage, *Chem. Eng. J.*, 2021, **406**, 126873.
10. S. Sui, H. Xie, M. Liang, B. Chen, C. Liu, E. Liu, B. Chen, L. Ma, J. Sha and N. Zhao, "Three-in-One" Multi-Level Design of MoS_2-Based Anodes for Enhanced Sodium Storage: from Atomic to Macroscopic Level, *Adv. Funct. Mater.*, 2022, **32**, 2110853.
11. Y. Wu, W. Zhong, Q. Yang, C. Hao, Q. Li, M. Xu and S.-j. Bao, Flexible MXene-$Ti_3C_2T_x$ bond few-layers transition metal dichalcogenides MoS_2/C spheres for fast and stable sodium storage, *Chem. Eng. J.*, 2022, **427**, 130960.
12. Z. Dong, X. Wu, D.-K. Cai, Q. Mao, K.-J. Huang, L. Wang and J. Xu, Interlayer-expanded MoS_2@C hollow nanorods for enhanced sodium storage, *Chem. Eng. Sci.*, 2022, **262**, 117976.
13. Z. Yuan, J. Cao, S. Valerii, H. Xu, L. Wang and W. Han, MXene-Bonded hollow MoS_2/Carbon sphere strategy for high-performance flexible sodium ion storage, *Chem. Eng. J.*, 2022, **430**, 132755.
14. J. Wu, J. Liu, J. Cui, S. Yao, M. Ihsan-Ul-Haq, N. Mubarak, E. Quattrocchi, F.

Ciucci and J.-K. Kim, Dual-phase MoS_2 as a high-performance sodium-ion battery anode, *J. Mater. Chem. A*, 2020, **8**, 2114-2122.

15. Y. Li, R. Zhang, W. Zhou, X. Wu, H. Zhang and J. Zhang, Hierarchical MoS_2 Hollow Architectures with Abundant Mo Vacancies for Efficient Sodium Storage, *ACS Nano*, 2019, **13**, 5533-5540.

16. C. Cui, Z. Wei, J. Xu, Y. Zhang, S. Liu, H. Liu, M. Mao, S. Wang, J. Ma and S. Dou, Three-dimensional carbon frameworks enabling MoS_2 as anode for dual ion batteries with superior sodium storage properties, *Energy Storage Mater.*, 2018, **15**, 22-30.